sustainability

MDPI

Article

Analysis of the Hydrochemical Characteristics and Genesis of Bosten Lake, China

Xiaolan Wang [1], Dilinuer Aji [1,2,*] and Saimire Tuoheti [1]

[1] School of Geography and Tourism, Xinjiang Normal Urumqi, Urumqi 830054, China
[2] Key Laboratory of Lake Environment and Resources in Arid area of Xinjiang, Urumqi 830054, China
* Correspondence: dilnur@xjnu.edu.cn; Tel.: +86-139-9994-0796

Abstract: The hydrogeochemical evolution of Bosten Lake has an important impact on the lake's ecology and water environment. Kriging interpolation, principal component analysis and Piper and Gibbs charts were used to analyze the hydrochemical characteristics and genesis of Bosten Lake in summer and autumn. The following are the main conclusions: (1) In summer and autumn, the hydrochemistry of the lake follows the order of $SO_4^{2-} > Cl^- > HCO_3^- > Na^+ > Mg^{2+} > Ca^{2+} > K^+$. (2) The concentrations of TDS, Ca^{2+}, Na^+, Mg^{2+}, Cl^- and HCO_3^- in Bosten Lake increased significantly in autumn. Ion concentrations in most of the Little Lake District were higher than those in the Great Lake District. (3) In summer, ion correlation was strong, the evaporation effect was strong and the TDS contribution rate was high. Evaporation was weak in autumn, and Mg^{2+} and Ca^{2+} contributed more. (4) The hydrochemical type (SO_4·Cl-Na·Mg) was the same in both seasons; in summer, the Great and Little lakes were mainly characterized by evaporation and crystallization; in autumn, evaporation crystallization was dominant in the Great lake. (5) The ions mainly came from the dissolution of gypsum, salt rock, calcite, etc. Cationic alternating adsorption occurred in summer.

Keywords: water chemistry; Piper trilinear diagram; kriging; Gibbs diagram; Bosten Lake

Citation: Wang, X.; Aji, D.; Tuoheti, S. Analysis of the Hydrochemical Characteristics and Genesis of Bosten Lake, China. *Sustainability* **2023**, *15*, 4139. https://doi.org/10.3390/su15054139

Academic Editor: Franco Salerno

Received: 26 December 2022
Revised: 21 February 2023
Accepted: 22 February 2023
Published: 24 February 2023

1. Introduction

Rivers and lakes are important water resources, indispensable for human life and production; they also facilitate the material and energy cycle between the land and ocean, and their hydrochemical properties have important implications for human health, aquatic biota and ecosystem services [1,2]. The chemical composition of water not only indicates surface weathering processes, but also reflects the source, composition and content characteristics of regional hydrochemical elements. The chemical properties of water bodies depend mainly on the chemical content of diagenetic minerals, such as sulfide, carbonates and silicate, and the physical effects of evaporation and weathering [3,4]. In recent years, some scholars have also conducted research on the water chemistry of lakes in semi-arid areas, and the research work on Bosten Lake has mainly focused on water quality [5,6], ecological service value [7,8] and lake area changes [9]. However, research on its water chemistry is relatively scarce. Nurameem Armuk studied the water chemistry of Bosten Lake using hydrogeochemical methods and isotopes, and came to the conclusion that the ion concentration in the Bosten Lake Basin was ordered and isotopes were evenly distributed in the lake [10].

Vernadcky first mentioned the water chemical composition of the Earth's rivers, and then many scholars analyzed the main solutes in the water chemistry of the basin. The relationship between its source and the environment of the region through which it flows was also analyzed. In 1970, Gibbs divided the factors affecting the water chemistry of the basin into three categories according to the chemical composition of the main solutes in the water body. This method is still widely used in the analysis of river chemistry [11]. Among those who have used this method are Prasanna et al., who used the hydrochemical

method to prove that groundwater and surface water around Perumal Lake in India are not affected by evaporation and precipitation, and the water bodies are not polluted except for a small part [12]. Mandal et al. investigated the groundwater in the Kingston Basin using hydrochemical methods to determine its hydrochemical type, confirming the contribution of saline invasion [13]. Zhang et al. studied the hydrochemistry of water bodies (Ili, Junggar and Erzis) in arid and semi-arid areas using the hydrochemical method, and it was proved that evaporative karst decomposition and carbonate weathering were the main causes of the hydrochemistry in these arid and semi-arid areas [14]. Wu Dingding et al., in addition to the hydrochemical method, used stable isotopes to study groundwater in Hami Basin, and it was concluded that the chemical type transformation of the groundwater and the main recharge mode are atmospheric precipitation, and the discharge mode is evaporation [15].

Principal component analysis was introduced by Karl Pearson in Britain and Harold Hotelling in the United States. In China, Professor Qiu Dong [16] has contributed greatly to principal component analysis (PCA), conducting long-term and in-depth research on PCA. Many experts and scholars [17] are also committed to the theoretical research of principal component analysis. The comprehensive evaluation of principal component analysis has been applied to many fields [18–21] such as medicine, education and environment. The following scholars have applied principal component analysis to the study of water chemistry. Lanjwani et al. used multivariate statistical methods and geochemical modeling (GIS map) to analyze the chemical composition and main ion sources of the groundwater of Bakrani Taluka in Pakistan [22]. Lu Ying, using multivariate statistical methods, studied groundwater chemistry in the Zhangye Basin and analyzed the hydrochemical characteristics of evaporation and concentration, recharge and leaching and acid–base evolution of the main loading variables at shallow and middle depths [23].

This study focuses on Bosten Lake as the research object, using Kriging interpolation, principal component analysis, Piper three-line graphs, Gibbs charts, and main ion ratio analysis to study the summer and autumn ion concentration characteristics, spatial distribution of ions and TDS, water chemical types and water chemical genesis of Bosten Lake, as well as the ion correlation and main sources. The findings will provide a reference basis for the assessment of the quality of local surface water, treatment and protection of the water environment, and the rational utilization of water resources.

2. Materials and Methods

2.1. Study Area

Bosten Lake is located in the Bayinggoleng Mongolian Autonomous Prefecture (Bazhou for short), Xinjiang Uygur Autonomous Region, in the northeast of Tarim Basin. The east and west sides are adjacent to the desert. Its geographical coordinates are between 82°57′–90°39′ E and 40°25′–43°21′ N (Figure 1). The drainage area is 7.73 × 104 km^2, accounting for 16.1% of the total area of Bazhou. The mountainous area is 3.47 × 104 km^2. The plain area is surrounded by deserts, and the ecological environment is extremely fragile [24].

The Bosten Lake Basin is a typical continental arid climate with little rain, and the temperature difference between morning and night is large, with large winds and sand. The annual precipitation in Bosten Lake Basin is in the range of 70–600 mm. The average annual evaporation is 1880.0–2785.8 mm, and the average annual temperature is 9.2–11.5 °C [9,25]. The Bosten Lake Basin is surrounded by mountains, high in the north and west, and low in the south and east [26].

It is the gathering place of rivers of all sizes in Yanqi Basin and there are 13 rivers in the basin. A total of 80% of its water flows in from the Kaidu River, and Bosten Lake is the source of the Kongque River, with the main flow-producing area being in the Tianshan Mountain system [27]. It is divided into two lakes, the main part of which is the Great Lake, and the main part of the small lake is a plurality of shallow moorings, located in the southwest corner of the Great Lake area. Surface tributaries and small lakes are connected

in series. The water levels in the flood period and the dry period are quite different, and the surface becomes dry during the dry period.

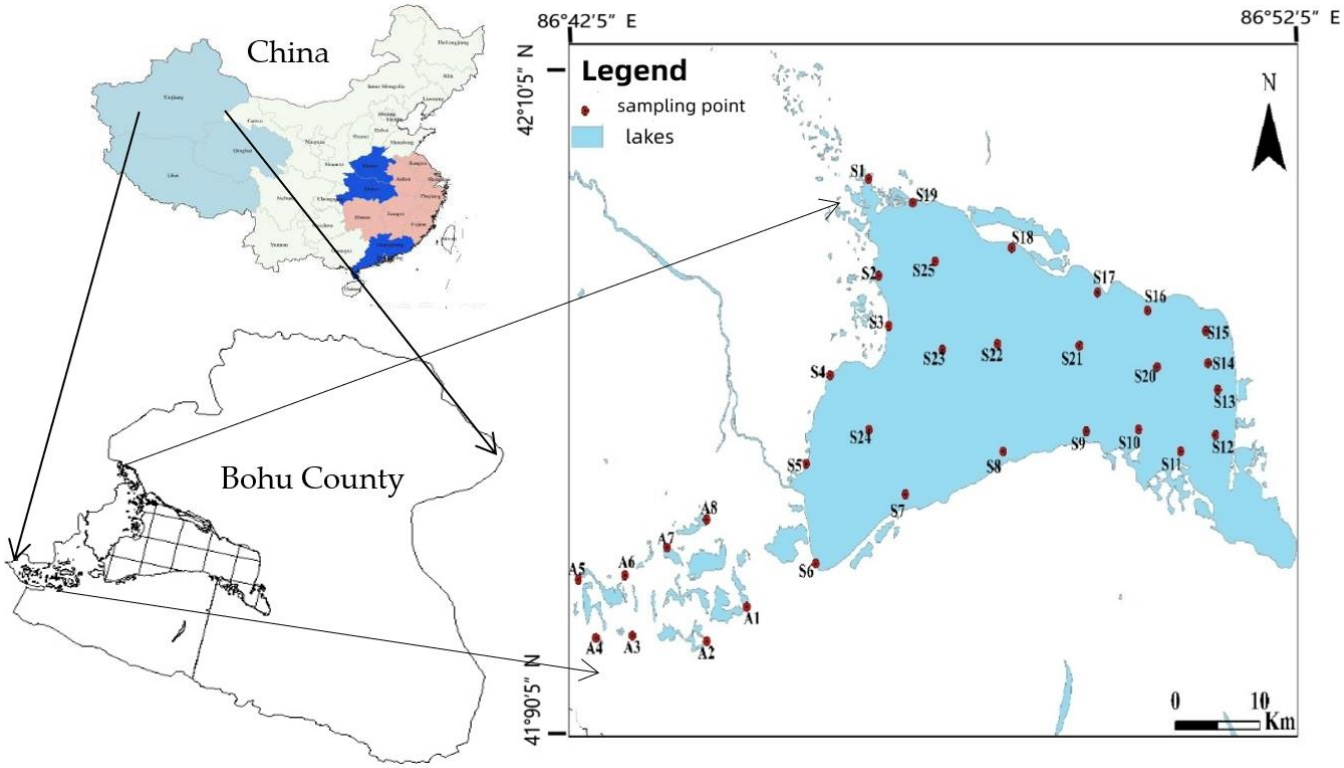

Figure 1. Overview of the study area.

There are many ethnic groups living in the Bosten Lake Basin, with a population of 1,179,700 as of 2019, including Han, Uyghur, Mongolian, Hui and Kazakhs. The increase in population and the development of science and technology have led to the rapid economic development of the basin, and the GDP of the basin reached CNY 106.13 billion in 2019, and the per capita GDP of the basin was CNY 62,749, of which the value of secondary industries was CNY 62.9 billion, accounting for 59.2% of the GDP, which is the leading industry in the economic development of the Bosten Lake Basin [28].

2.2. Acquisition and Testing of the Water Samples

In the summer and autumn of 2021 (in the northern hemisphere of China, June represents summer and October represents autumn), water samples were collected and monitored for HCO_3^-, SO_4^{2-}, Cl^-, K^+, Ca^{2+}, Na^+ and Mg^{2+}. The samples were collected from 33 sampling points covering the Great and Little lakes of Bosten Lake: 25 sampling points (S1–S25) in the Great Lake District and 8 sampling points (A1–A8) in the Little Lake District. Golden Beach, Silver Beach, Dahekou, and other scenic spots and factories around Bosten Lake are greatly affected by human activities. Therefore, 20 sampling points were set around the lake and 5 sampling points were set in the center of the lake, which is less affected by human activities, to ensure the accuracy and equality of data. The Little Lake District has a small scope and is a reed breeding area, so setting 8 sampling points can achieve full coverage and make the data representative. The samples were collected at 0.5 m below the water surface in the center of the lake using a boat. They were stored in transparent polyethylene bottles, which were preliminarily washed thrice and subsequently marked. Three samples were collected from each point. The collection, preservation and delivery of samples were performed in accordance with standards. Field measurements of the pH (generally refers to the hydrogen ion concentration index and value of acidity or alkaline of the solution) of water samples collected on the day was performed using an

8601 AZ pH meter. TDS (total dissolved solids) and conductivity were measured using a handheld conductivity meter. Laboratory determinations included the following: HCO_3^- was measured by acid titration; SO_4^{2-} and Cl^- were measured by ion chromatography; K^+ and Na^+ were measured by flame atomic absorption spectrophotometry; and Ca^{2+} and Mg^{2+} were measured by atomic absorption spectrophotometry [29,30].

2.3. Research Method

Statistical analysis was performed using Microsoft Excel and the variability of the data was tested using the Yin–Yang ion balance method. The calculation showed that the absolute value of the ion balance error was less than 5% or less for all water samples [31]. Spatial interpolation was performed using the kriging interpolation method, and the homology between various ions was assessed through correlation analysis. The Piper trilinear diagram and Gibbs plots were drawn using Origin software and major ion ratio and the alternating adsorption of the cations were considered to study the chemical characteristics and evolution of the hydrochemistry of Bosten Lake.

Kriging interpolation is also known as the most optimal interpolation method of spatial self-covariance. The ordinary kriging interpolation, which is expressed as Equation (1), assumes few conditions and simple parameter requirements, which is one of the most common grounds in statistical methods. Based on raw data and the characteristics of the various functions, it performs a linear, unbiased, optimized estimation of unknown sample points in limited regions [29,30].

$$P(x_0) = \sum_{i=1}^{n} \lambda_i P(x_i) \quad (1)$$

In the formula, $P(x_0)$ is the predicted value of the water quality index, λ_i is the weight of the ith sampling point to the interpolation point, n is the number of measured sampling points, and the ith sampling point of $P(x_i)$.

Principal component analysis (PCA) uses dimension reduction thinking to convert multiple variables into a few variables, and these comprehensive variables can reflect most of the information provided by the original variables. In this study, principal component analysis was used to extract the dominant ions and variables in water chemistry and convert multiple indicators into a few comprehensive indicators. The dominant ion contribution rate to the water chemistry in summer and autumn was analyzed. The steps are as follows: standardize the original data; establish the relationship matrix; calculate the eigenvalues and eigenvectors of the correlation coefficient matrix; and calculate the comprehensive score [32,33].

3. Results

3.1. Characteristics of the Hydrochemical Parameters

The results of the statistical analysis of chemical index data are presented in Tables 1 and 2. The cation and anion concentrations followed the order $Na^+ > Mg^{2+} > Ca^{2+} > K^+$ and $SO_4^{2-} > Cl^- > HCO_3^-$, respectively, in both summer (June) and autumn (October). In summer, the average cation mass concentrations were 134.47 (Na^+), 48.26 (Mg^{2+}), 32.29 (Ca^{2+}) and 12.39 mg/L (K^+), and the average anion mass concentrations were 404.35 (SO_4^{2-}), 253.21 (Cl^-) and 203.5 mg/L (HCO_3^-). In autumn, the average cation mass concentrations were 153.67 (Na^+), 50.72 (Mg^{2+}), 44.48 (Ca^{2+}) and 11.9 mg/L (K^+), and the average anion mass concentrations were 422.3 (SO_4^{2-}), 257.18 (Cl^-) and 168.33 mg/L (HCO_3^-). On the whole, the ionic concentrations followed the same order between summer and autumn: $SO_4^{2-} > Cl^- > HCO_3^- > Na^+ > Mg^{2+} > Ca^{2+} > K^+$.

Table 1. Hydrochemical parameters of the lake water during summer and autumn. pH is dimensionless; TDS is in ppm; the other indicators are in mg/L.

	Statistical Value	pH	TDS	K^+	Na^+	Ca^{2+}	Mg^{2+}	Cl^-	SO_4^{2-}	HCO_3^-
Summer	Maximum value	7.74	960	23.1	621	91.1	184	1190	1520	854
	Minimum value	7.05	481	1.54	7.73	15.0	9.02	11.9	32.6	95.5
	Mean value	7.49	671.79	12.39	134.47	32.29	48.26	253.21	404.35	203.5
	Standard deviation	0.14	115.24	6.87	115.47	17.47	30.96	236.53	310.41	147.75
Autumn	Maximum value	8.52	893	73.9	971	103	146	545	988	198
	Minimum value	7.37	228	1.35	8.24	12.9	11.3	109	215	117
	Mean value	8.06	707.46	11.99	153.67	44.48	50.72	257.18	422.3	168.33
	Standard deviation	0.40	115.42	11.17	161.58	17.32	21.34	110.91	166.94	14.62

Table 2. Hydrochemical parameters of the Great and Little lake areas in summer and autumn. pH is dimensionless; TDS is in ppm; the other indicators are in mg/L.

		Statistical Value	pH	TDS	K^+	Na^+	Ca^{2+}	Mg^{2+}	Cl^-	SO_4^{2-}	HCO_3^-
Summer	**Great Lake District**	Maximum value	7.69	960	44.4	373	61.1	101	763	963	557
		Minimum value	7.16	596	1.54	7.73	15.0	9.02	11.9	32.6	95.5
		Mean value	7.52	729.6	12.89	123.87	27.54	42.02	205.88	341.34	174.66
		Standard deviation	0.11	60.92	7.00	57.57	8.02	14.01	120.03	147.63	80.21
	Little Lake District	Maximum value	7.74	507	23.1	621	91.1	184	1190	1520	854
		Minimum value	7.05	481	6.82	22.5	25.0	27.1	102	183	150
		Mean value	7.40	491.13	10.82	167.59	47.11	67.74	401.13	601.25	293.63
		Standard deviation	0.19	9.82	6.17	207.84	27.73	53.29	396.07	527.42	243.35
Autumn	**Great Lake District**	Maximum value	8.52	893	73.9	971	103	146	359	591	186
		Minimum value	7.43	627	7.86	79.3	29.4	38.6	149	253	153
		Mean value	8.17	758.4	12.77	135.9	40.1	49.27	216.72	354.4	167.08
		Standard deviation	0.38	41.19	12.53	171.34	13.39	19.97	35.44	56.76	8.50
	Little Lake District	Maximum value	8.05	657	13.8	331	81.7	85.8	545	988	198
		Minimum value	7.37	228	1.35	8.24	12.9	11.3	109	215	117
		Mean value	7.72	548.25	9.53	209.21	58.18	55.24	383.63	634.5	172.25
		Standard deviation	0.20	127.25	3.99	109.04	20.72	24.59	160.35	213.21	25.22

In summer, the pH of the Great Lake District was 7.52 and that of the Little Lake District was 7.40, indicating weakly alkaline water in both districts. In autumn, the pH of the Great Lake District was 8.17 and that of the Little Lake District was 7.72, indicating alkaline water in the Great Lake District and weakly alkaline water in the Little Lake District. In summer, the overall pH of the surface water in the study area ranged from 7.05

to 7.74, with a mean of 7.49; in autumn, it ranged from 7.37 to 8.52, with a mean of 8.06. This indicates that Bosten Lake is the most alkaline in autumn. In summer, TDS ranged from 596 to 960 ppm (Great Lake District), with a mean of 729.6 ppm, and from 481 to 507 ppm (Little Lake District), with a mean of 491.13 ppm. In autumn, TDS ranged from 627 to 893 ppm (Great Lake District), with a mean of 758.4, and from 228 to 657 ppm, with a mean of 548.25 (Little Lake District). Overall, the mean TDS of the surface water in the study area was 671.79 ppm in summer and 707.46 ppm in autumn. Both pH and TDS were higher in autumn than in summer and also higher in the Great Lake District than in the Little Lake District.

3.2. Spatial Distribution of the Ions and the TDS

TDS can represent the comprehensive characteristics of solute quality in water. It is relatively complicated to analyze ions alone. In addition, TDS and conductivity are strongly related, and pH and water temperature do not show distinct features.

According to the spatial interpolation change in TDS in the study area (Figure 2o,p), the spatial distribution of Bosten Lake's TDS in summer and autumn varied greatly. The spatial distribution map of TDS shows that TDS content was the lowest in summer (Figure 2o), with that of the lakeside below Bosten Lake being greater than that above. An area of high TDS content could be observed around the highest value on the southern right part, surrounding the desert. This distribution indicates that the lake's water body has a low content of dissolved materials in summer. In autumn (Figure 2p), the TDS content was low in the Little Lake District, and the overall TDS content was high in the Great Lake District, with two high-TDS areas. This indicates a high content of dissolved materials in autumn.

In summer, the maximum Ca^{2+} concentration was found in the Little Lake District, while the overall concentration in the Great Lake District was low. The Ca^{2+} concentration in the Bosten Lake area showed a decreasing trend from bottom to top. In autumn, the overall temperature of the Little Lake District decreased, while that of the Egret Lake area of the Great Lake District reached the highest value. Ca^{2+} concentration in the upper left area of the Great Lake District was moderate and the ion distribution was relatively dispersed.

In summer, the concentration of K^+ ions showed an extreme value, and the maximum value appeared in the lower left part of the lake. Moreover, the concentration of K^+ in the lakeside below Bosten Lake was medium to high, showing a decreasing spatial distribution from bottom to top, and the concentration in the Little Lake District was low as a whole. In autumn, there was an extreme value of K^+ concentration in the Great and Little Lake District, while the concentration in the center of the Great Lake District was low, and the overall concentration was low and had a maximum value.

In summer, Na^+ was generally low, and Na^+ was on the high side where Kaidu River enters the lake. The concentration of Na^+ was low in the entire Great Lake District, and there was no extreme value in the Little Lake District. The overall spatial distribution of Na^+ decreased from the middle to both sides. In autumn, the concentration of Na^+ in the center of the extreme lake was low in the Great Lake District, while the concentration of Na^+ in the Little Lake District was high.

In summer, Mg^{2+} was low, the concentration of Mg^{2+} at the entrance of Kaidu River was high, and the concentration of Mg^{2+} in the Little Lake District was high. In autumn, the Mg^{2+} concentration was higher as a whole, while lower in the center of the lake, with two maximum values. As can be seen from the figure, the concentration of Mg^{2+} around the Great Lake District was high and appeared to be an extreme value, while the Little Lake District presented a trend of gradual decline from left to right.

In summer, Cl^- concentration was lower in the Great Lake area, the lowest value was found at the entrance of the Kaidu River, the lower value was higher, and the highest value was found in the Little Lake District, decreasing from top to bottom. In autumn, the overall Cl^- concentration was higher, and the concentration of Cl^- was lower in the center of the lake, showing the maximum value in the upper right. The overall concentration of Cl^- was the highest in the Little Lake District, decreasing from left to right.

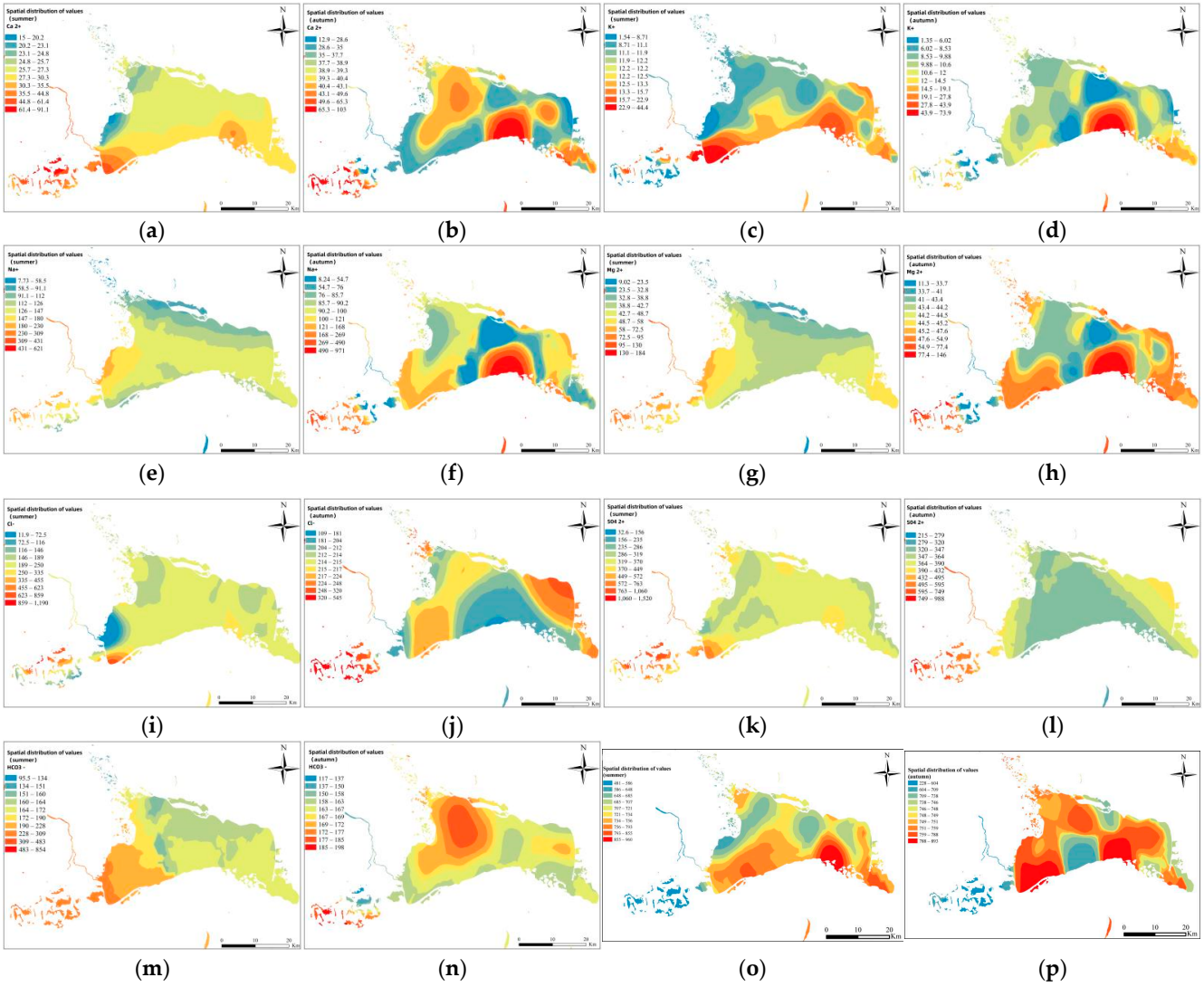

Figure 2. Spatial distribution of TDS. (**a**,**c**,**e**,**g**,**i**,**k**,**m**,**o**) represents summer and (**b**,**d**,**f**,**h**,**j**,**l**,**n**,**p**) represents autumn, where blue represents the minimum value range and red represents the maximum value range.

In summer, the concentration of SO_4^{2-} in the Little Lake District was the extreme value, and the overall concentration of SO_4^{2-} in the Little Lake District was high, while the overall concentration of SO_4^{2-} in the Great Lake District was low. In autumn, the concentration of SO_4^{2-} in the small lake area increased, while the concentration of SO_4^{2-} in the Great Lake District decreased, and most of areas had decreased concentrations of SO_4^{2-}, mainly in the Little Lake District.

In summer, HCO_3^- was higher in the Little Lake District, but lower in the Great Lake District as a whole, and the HCO_3^- content was higher in the Great Lake District where the Kaidu River entered the lake mouth. In autumn, the extreme value appeared in the Little Lake District, and the HCO_3^- concentration increased in the Little Lake District. The overall HCO_3^- concentration increased in the Little Lake District, and the HCO_3^- concentration markedly increased above.

3.3. Ion Source

The relationship and source of ions can be roughly deduced through correlation analysis (Table 3). For summer, a very significant correlation was observed between Mg^{2+} and Cl^-, SO_4^{2-}, Na^+ and HCO_3^-, with large correlation coefficients. Regarding autumn, significant negative correlations were observed between TDS and SO_4^{2-} and K^+,

with correlation coefficients of 0.483 and 0.381, indicating that the two ions contributed significantly to TDS. Further, the correlation coefficient of SO_4^{2-} was greater than that of K^+, indicating that the contribution of SO_4^{2-} played a decisive role in autumn.

Table 3. Matrix of the correlation coefficient of water chemical parameters in summer and autumn.

		HCO_3^-	Cl^-	SO_4^{2-}	K^+	Na^+	Ca^{2+}	Mg^{2+}	pH
Summer	Cl^-	0.944 **							
	SO_4^{2-}	0.893 **	0.985 **						
	K^+	0.707 **	0.665 **	0.620 **					
	Na^+	0.911 **	0.961 **	0.943 **	0.684 **				
	Ca^{2+}	0.824 **	0.924 **	0.955 **	0.545 **	0.835 **			
	Mg^{2+}	0.945 **	0.987 **	0.971 **	0.631 **	0.967 **	0.889 **		
	PH	0.012	−0.065	−0.131	0.104	0.101	−0.342	0.002	
	TDS	−0.265	−0.29	−0.272	0.204	−0.103	−0.358 *	−0.275	0.211
Autumn	Cl^-	0.468 **							
	SO_4^{2-}	0.136	0.889 **						
	K^+	0.02	−0.073	−0.142					
	Na^+	0.156	0.279	0.206	0.920 **				
	Ca^{2+}	0.392 *	0.582 **	0.482 **	0.651 **	0.830 **			
	Mg^{2+}	0.15	0.350 *	0.292	0.843 **	0.927 **	0.875 **		
	PH	0.022	−0.199	−0.268	−0.217	−0.307	−0.367 *	−0.263	
	TDS	0.222	−0.245	−0.0483 **	0.381 *	0.178	0.045	0.318	0.315

Pour: ** $p < 0.01$ (There was a significant correlation), * $p < 0.05$ (There is a weak correlation).

According to the correlation analysis, Mg and Na generally show a strong correlation and have similar sources. The Cl/Na value was 1.88 in summer and 1.67 in autumn, which are higher than the ratio for global seawater (Cl/Na = 1.15). This shows that the salt brought by atmospheric circulation has an important contribution to the chemical composition of the lake water, with a higher contribution in summer. K^+ is generally derived from the weathering of minerals such as mica and potassium feldspar. The K/Na ratio of the lake water was 0.089 and 0.078 in summer and autumn, respectively, with an average of 0.084, indicating that some potassium feldspar may not be completely weathered (low degree of weathering). HCO_3^- and Mg^{2+} are mainly derived from the dissolution of carbonate. The correlation coefficient of SO_4^{2-} with Ca^{2+} was 0.955 in summer and 0.482 in autumn, indicating that, in addition to the strong weathering in summer, some gypsum dissolution occurred, mainly derived from human activity. In autumn, Ca^{2+}, as the main cation of the lake water, indicates that calcium feldspar weathering is also the main weathering process in the region.

Prior to principal component analysis, KMO and Bartlett tests were performed on the data. As shown in Table 4, the KMO value was 0.674, greater than 0.5, and the significance level was 0.000, less than 0.05, indicating that the data could be analyzed by principal component analysis. The principal component analysis method was used to extract two principal components with eigenvalues greater than 1, and the cumulative variance contribution rate was 87.445%, indicating that the two principal components could reflect 87.445% of the original information of the 18 indicators. The results of the principal component analysis were good, and the two principal components were named F1 and F2.

Table 4. KMO and Bartlett's tests.

Kaiser–Meyer–Olkin Measure of Sampling Adequacy		0.674
Bartlett's Test of Sphericity	Approx. chi-squared	1220.246
	df	153
	sig	0.000

The angle between the lines represents the correlation, and the smaller the angle, the closer the correlation. If the angle between two lines is greater than 90 degrees, the correlation is small and the correlation is negative. In the principal component diagram, the longer the indicator arrow, the greater the contribution rate of the indicator. It can be seen from the figure that, in summer (Figure 3a), there was a strong correlation and positive correlation among all ions. F1 was the main ion, and its contribution rate reached 62.8%, indicating that F1 was subject to strong evaporation. F2 only had a contribution rate of 21.9%, which was less affected. TDS had a positive correlation with a small number of ions, among which TDS was the main contributor. In autumn (Figure 3b), there was a strong and positive correlation among all ions. F1 was the main ion, but its contribution rate was 40.7%, indicating that the evaporation effect was weakened in autumn. The F2 contribution rate was 30.1%, not considerably different from F1. TDS had a positive correlation with most ions, among which Ca^{2+} and Mg^{2+} contributed the most.

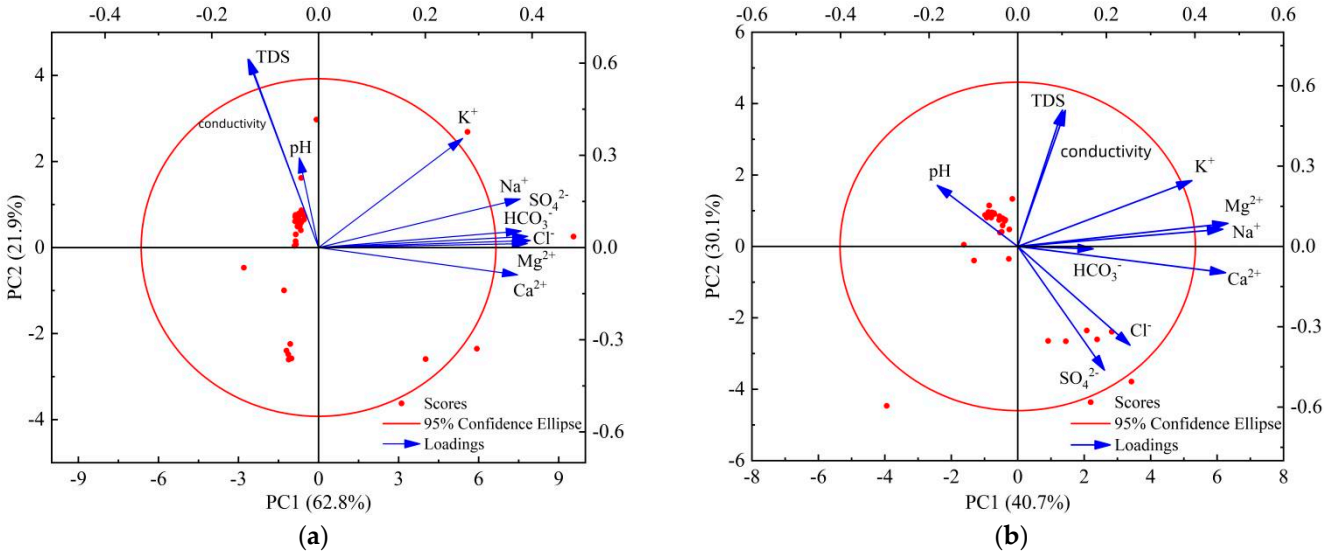

Figure 3. PCA. (**a**) represents summer and (**b**) represents autumn.

3.4. Hydrochemical Type

The Piper diagram can indicate the chemical composition characteristics of different water samples, expressed as the milligram equivalent percentage of the main cations and anions (Figure 4). In summer (Figure 4a), the main distribution of cations in Bosten Lake was biased towards the Na^++K^+ axis, and the anion distribution was biased towards SO_4^{2-}. In the Great Lake District, Na^++K^+, Ca^{2+} and Mg^{2+} accounted for 53.9%, 13% and 33.1% of all cations, respectively, and HCO_3^-, SO_4^{2-} and Cl^- accounted for 16.9%, 49.5% and 33.6% of all anions, respectively. The hydrochemical type mainly corresponded to SO_4·Cl-Na·Mg. In the Little Lake District, Na^++K^+, Ca^{2+} and Mg^{2+} accounted for 48.6%, 15.1% and 36.3% of all cations, respectively, and HCO_3^-, SO_4^{2-} and Cl^- accounted for 15.7%, 48.1% and 36.2% of all anions, respectively. The hydrochemical type mainly corresponded to SO_4·Cl-Na·Mg. In autumn (Figure 4b), the main distribution of cations in the Great Lake District was biased towards the Na^++K^+ axis, and the anion distribution was biased towards SO_4^{2-}. In the Great Lake District, Na^++K^+, Ca^{2+} and Mg^{2+} accounted for 50.6%, 16.2% and 33.2% of all cations, respectively, and HCO_3^-, SO_4^{2-} and Cl^- accounted for 15.7%, 49.9% and 34.4% of all anions, respectively. The hydrochemical type mainly corresponded to SO_4·Cl-Na·Mg. In the Little Lake District, Na^++K^+, Ca^{2+} and Mg^{2+} accounted for 55.4%, 17.3% and 27.3% of all cations, respectively, and HCO_3^-, SO_4^{2-} and Cl^- accounted for 9.7%, 53.7% and 36.6% of all anions, respectively. The hydrochemical type mainly corresponded to SO_4·Cl-Na·Mg. Overall, in summer and autumn, the same hydrochemical types were observed in the Great and Little Lakes (SO_4·Cl-Na·Mg). According to the analysis of water sample data in summer and autumn, Na^+ content was the highest among cations, followed by Mg^{2+},

and the SO_4^{2-} content was the highest among anions. The hydrochemical type indicates that the lake water will generally follow the evolution law of sodium carbonate–sulfate–magnesium sulfate–chloride type [34,35]. Accordingly, it can be determined that Bosten Lake is in the middle and late stage of evolution and that it is a relatively mature lake.

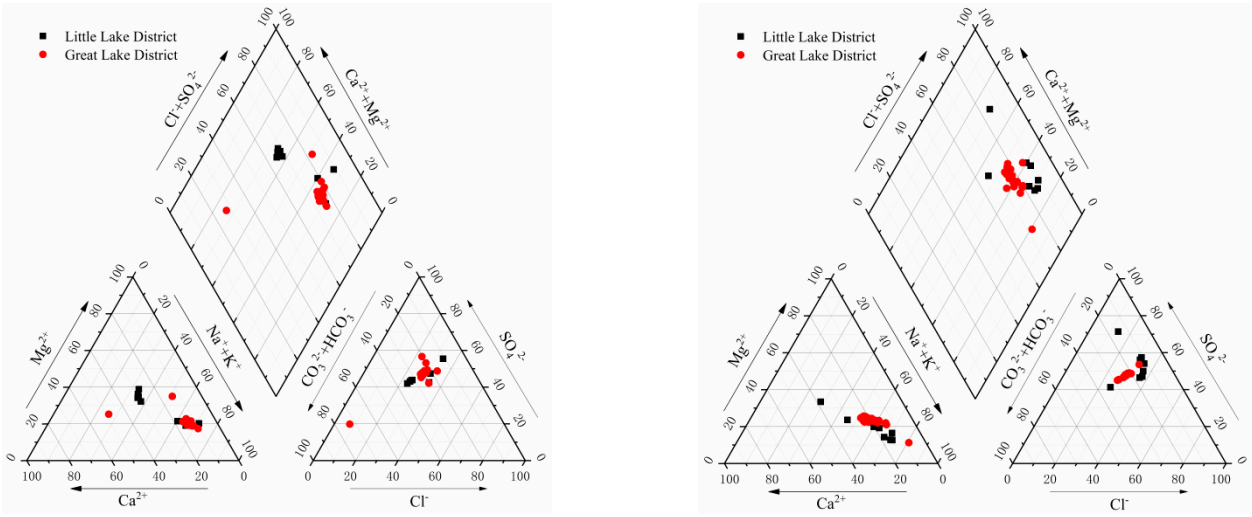

Figure 4. Piper diagram of the major ions in summer and autumn. (**a**) represents summer and (**b**) represents autumn. The black dots represent the Little Lake District values and the red dots represent the Great Lake District values.

3.5. Hydrochemical Evolution

The Gibbs diagram can be used to intuitively evaluate the chemical composition, formation, cause and mutual relationship of the components of lake water (Figure 5). The vertical coordinates are the logarithmic coordinates of TDS mass concentration in the river water, and the normal coordinates represent the ratio of the main cations $Na^+/(Na^+{+}Ca^{2+})$ or the main anions $Cl^-/(Cl^-{+}HCO_3^-)$. The Gibbs diagram divides factors affecting the chemical components of lake water into three aspects: evaporation and crystallization, rock weathering, and atmospheric precipitation. On the whole, for the summer and autumn, water sample points were mostly distributed in the middle and upper parts of the figure, with higher TDS contents (mostly 400–1000). The $Na^+/(Na^+{+}Ca^{2+})$ or $Cl^-/(Cl^-{+}HCO_3^-)$ ratios were distributed equally between 0.2 and 0.9. This shows that various ions in Bosten Lake were essentially derived from evaporative crystallization, with a very small part derived from rock weathering. Precipitation had almost no effect. In addition, most chemical components of the water samples were distributed within the Gibbs diagram, but a small number of water samples occurred outside the Gibbs plot. This shows that the hydrochemical components were also affected by the monsoon climate and anthropogenic interference to some extent.

For summer (Figure 5a,b), the ratio of Yin and Yang ions was 0.3–0.9, and the TDS range was 400–1000, indicating that the chemical components in the Bosten Lake are mainly derived from evaporation crystallization, with a small contribution from rock weathering. For autumn (Figure 5c,d), the cation distribution was scattered and slightly to the right, indicating that evaporation crystallization has a larger contribution compared to rock weathering. A cation distribution shifting to the left indicates that evaporation crystallization has a lower contribution than rock weathering. The anion distribution in the lake area showed that the hydrochemical in the Bosten Lake was affected by evaporation and crystallization, rock weathering and human activities. The cation ratio was greater than the anion ratio, indicating that the Yin and Yang ions have distinctly different sources.

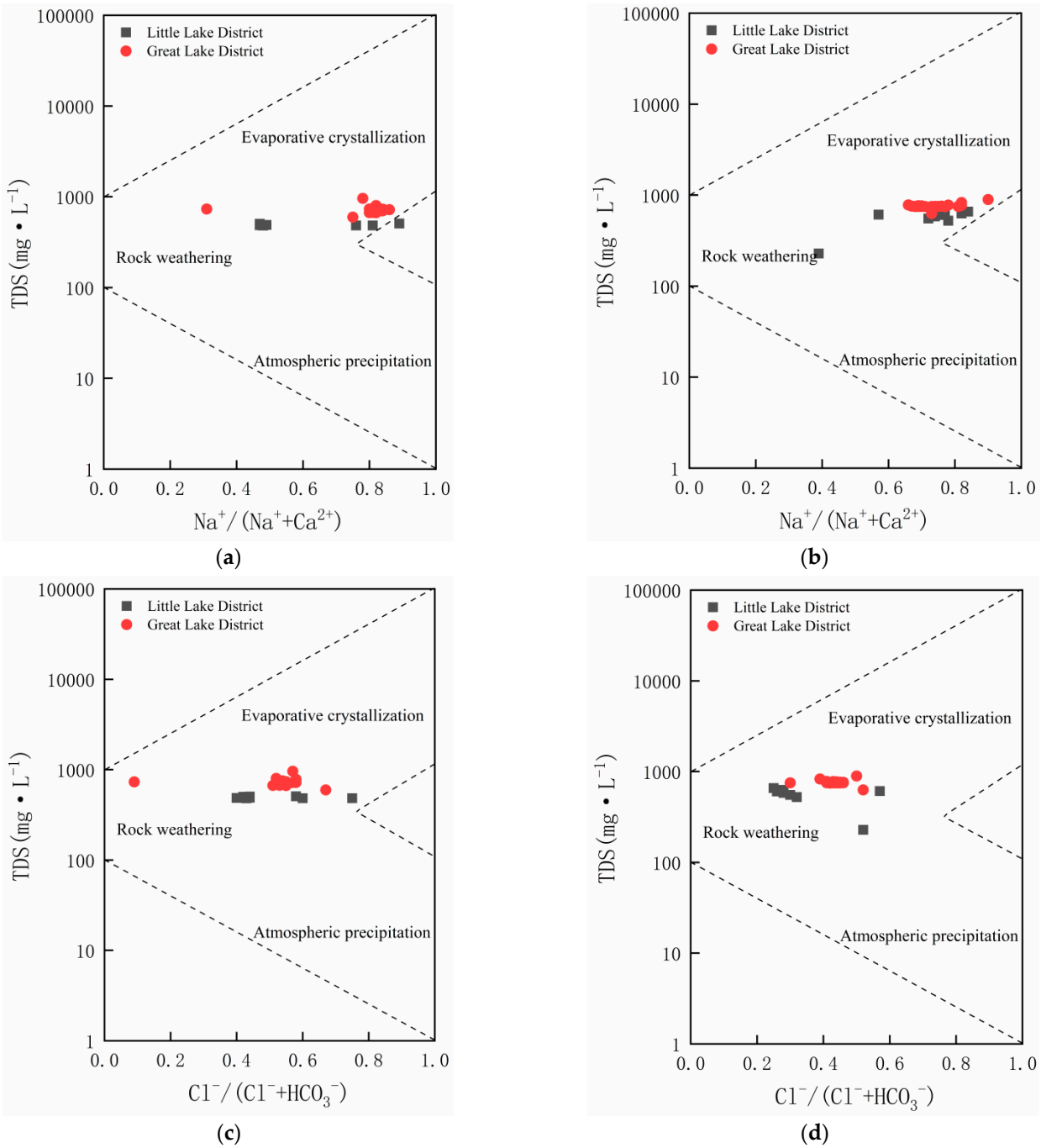

Figure 5. Gibbs plot of the chemical components of Bosten Lake in summer and autumn. (**a**,**b**) represent summer; (**c**,**d**) represent autumn. The black dots represent the Little Lake District values and the red dots represent the Great Lake District values.

3.6. Main Ion Ratio

To explore the water chemistry of Lake Bosten, the ratio diagram of main ions was drawn to illustrate the source of ions and the relationship between ions.

In the Ca^{2+}/SO_4^{2-} figure, the 1:1 line represents the gypsum and anhydrite dissolution line. In Figure 6a,b, the water samples of Bosten Lake in summer are distributed below the 1:1 line, which indicates the presence of Ca^{2+} and SO_4^{2-} in the water body, except from gypsum dissolution, and the excess in SO_4^{2-} may come from other sulfuric acid mineral dissolution. The water samples in autumn were generally distributed around the 1:1 line, indicating that the main source of Ca^{2+} and SO_4^{2-} in the water was gypsum dissolution.

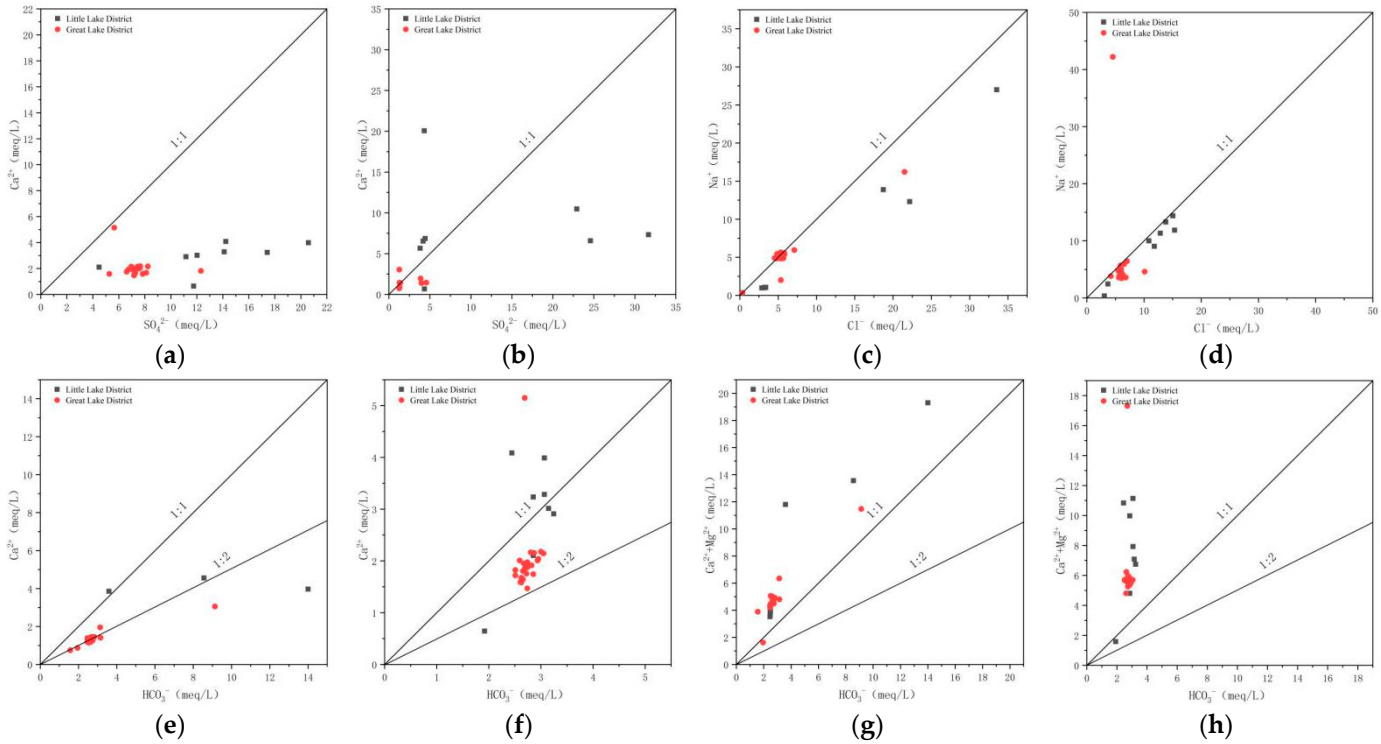

Figure 6. Ion ratio plot. (**a**,**c**,**e**,**g**) is the summer ion ratio and (**b**,**d**,**f**,**h**) is the autumn ion ratio. The black dots represent the Little Lake District values, and the red dots represent the Great Lake District values.

In the Na^+/Cl^- figure, the 1:1 line represents the dissolution line of salt rock. In Figure 6c,d, the water sample points in both Great and Little Lake Districts of Bosten Lake in summer and autumn were distributed on the 1:1 line, indicating that Na^+ and Cl^- in water bodies in summer and autumn mainly came from the dissolution of salt rock.

Regarding $(Ca^{2+}+Mg^{2+})/(HCO_3^-+SO_4^{2-})$, the 1:1 line represents the dissolution line of gypsum, aragonite, calcite and dolomite. It can be seen from Figure 6e,f that the water sample points of Bosten Lake in summer and autumn were all at 1:1 below the line, which indicates that the Ca^{2+}, Mg^{2+}, HCO_3^- and SO_4^{2-} in the water body mainly came from the dissolution of gypsum, calcite and dolomite, and the excess in SO_4^{2-} came from the dissolution of other sulfuric acid minerals.

In the Ca^{2+}, Mg^{2+} and HCO_3^- plots, the lake area points of Bosten Lake were distributed above the 1:1 line for $(Ca^{2+}+Mg^{2+})/HCO_3^-$ plots (Figure 6g,h), which indicates that Ca^{2+}, Mg^{2+} and HCO_3^- in the two seasons came from the dissolution of other calcium-containing minerals in addition to the dissolution of calcite and dolomite. In summer, the water samples in Bosten Lake and Little Lake District were distributed on the Ca^{2+}/HCO_3^- 1:2 line (Figure 6e,f), indicating that the ions in summer water mainly came from the dissolution of aragonite and calcite, while the water samples in autumn were distributed between 1:1 and 1:2, indicating that the ions in autumn mainly came from the dissolution of dolomite and calcite.

Alternating cation adsorption is one of the important links of water–rock interactions and also an indispensable part of the water cycle evolution process. By drawing the relationship between $(Na^+ + K^+ - Cl^-)$ and $(Ca^{2+}+Mg^{2+})-(HCO_3^-+SO_4^{2-})$ in Bosten Lake in summer and autumn, the cationic alternating adsorption of Bosten Lake water samples in two seasons can be analyzed (Figure 7).

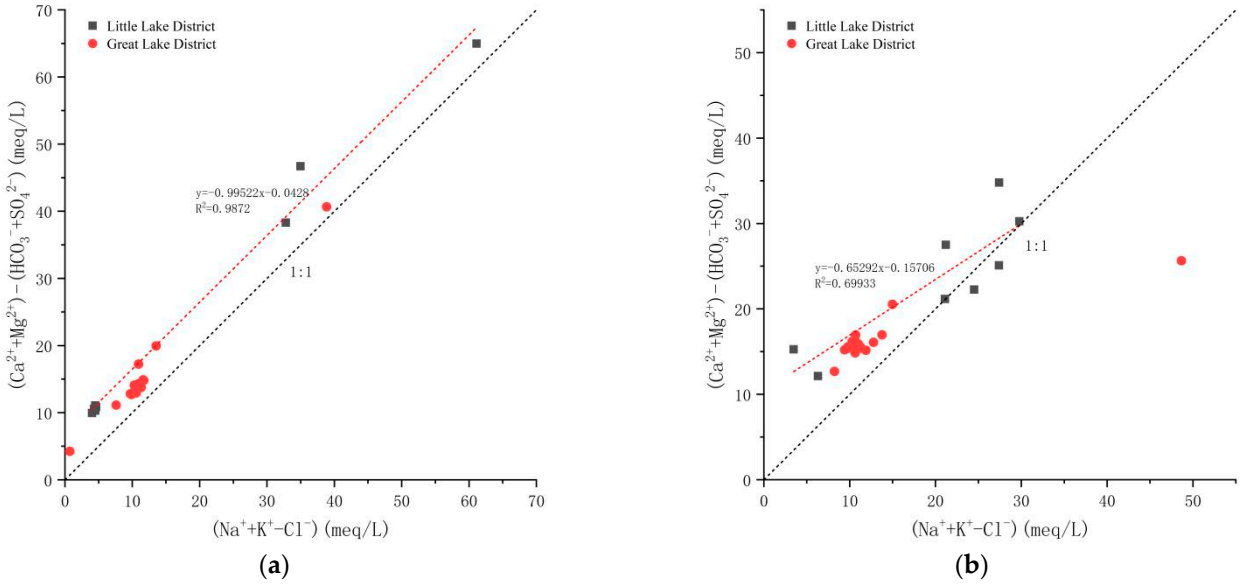

Figure 7. Cation replacement plots. (**a**) represents the alternating cation adsorption diagram of Bosten Lake in summer, (**b**) represents the adsorption diagram of alternating cations in Bosten Lake in autumn. The black dots represent the Little Lake District values, and the red dots represent the Great Lake District values.

In the cation alternate adsorption diagram, the difference in (Na^++K^+-Cl^-) represents the decrease or increase in Na^+ caused by other minerals except from salt rock dissolution, and the difference in (Ca^{2+}+Mg^{2+})-(HCO_3^-+SO_4^{2-}) represents the decrease or increase in Ca^{2+} and Mg^{2+} caused by other minerals except from the dissolution of gypsum and other conventional minerals. A slope close to −1 indicates that cationic alternating adsorption occurs in the water sample.

Figure 7a shows that the water samples of Bosten Lake in summer are all near the 1:1 line, and the ratio of (Na^++K^+-Cl^-) to (Ca^{2+}+Mg^{2+})-(HCO_3^-+SO_4^{2-}) is as follows: $y = -0.99522x - 0.0428$; the slope of the equation is −0.99522, which is infinitely close to −1; and $R^2 = 0.9872$, indicating that the cation alternating adsorption occurred and Na^+ mainly came from the dissolution of salt rock. In autumn (Figure 7b), the water samples of Bosten Lake and other lakes are relatively close to the 1:1 line, but the ratio of (Ca^{2+}+Mg^{2+})-(HCO_3^-+SO_4^{2-}) is $y = -0.65292x - 0.15706$, the slope is −0.65292, not close to −1, and $R^2 = 0.69933$, indicating that the cation alternating adsorption was weak and Ca^{2+} and Mg^{2+} had other sources. As can be seen from the alternating cation adsorption diagram in summer and autumn, the alternating cation adsorption in the Bosten Lake water body in summer was greater than that in autumn. The content of Na^+ in the Bosten Lake water body in summer increased, while the content of Ca^{2+} and Mg^{2+} was reduced. In autumn, Na^+ was decreased, while Ca^{2+} and Mg^{2+} were increased.

The following results were obtained from this study. Judging from the water chemical parameters, overall, the trend of ion concentrations remained the same in summer and autumn, following the order of $SO_4^{2-} > Cl^- > HCO_3^- > Na^+ > Mg^{2+} > Ca^{2+} > K^+$, and anions were more dominant in the lakes. However, in summer, the pH value of the Great Lake District was higher than that of the Little Lake District, and the entire lake was weakly alkaline. In autumn, the pH value of the Great Lake District was higher than that of the Little Lake District, which was alkaline. According to the pH value of Bosten Lake, the pH was higher in autumn, and the lake water was weakly alkaline. According to the spatial distribution map, the concentrations of TDS, Ca^{2+}, Na^+, Mg^{2+}, Cl^- and HCO_3^- in Bosten Lake increased significantly in autumn, while the concentrations of K^+ and SO_4^{2-} decreased. The ion concentrations in most of the Little Lake District were higher than those in the Great Lake District. The correlation analysis and PCA showed that the correlation between ions in autumn was lower than that in summer, but both were positively correlated.

The evaporation effect was strong in summer, and the contribution rate of TDS was high. In autumn, the evaporation was weakened, and Mg^{2+} and Ca^{2+} contributed more. In summer and autumn, Na^{+} had the highest content among all cations, followed by Mg^{2+}, and $SO_4{}^{2-}$ which had the highest content among anions. Moreover, the hydrochemical type (SO_4·Cl-Na·Mg) was the same throughout the lake and in both seasons. Accordingly, Bosten Lake is in the middle and late stages of evolution and is a relatively mature lake. The Gibbs plot analysis showed that, in summer, the Great and Little lakes were mainly characterized by evaporation and crystallization, with some rock weathering; in autumn, evaporation crystallization was dominant in the Great lake, whereas rock weathering was dominant in the Little lake. On the whole, the Great and Little lakes were affected by evaporation crystallization, rock weathering and human activities; according to the ratio of major ions, summer ions mainly came from the dissolution of gypsum, salt rock, calcite, dolomite and aragonite, and the excess in Ca^{2+} and $SO_4{}^{2-}$ had other sources. The autumn ions originated mainly from the dissolution of gypsum, salt rock, calcite and dolomite, and the excess in Ca^{2+} had other sources. Cationic alternating adsorption occurred in summer and the content of Na^{+} increased, while the content of Ca^{2+} and Mg^{2+} decreased. The opposite occurred in autumn.

4. Discussion

The main ionic characteristics of watershed water chemistry as a major tool to study the process of chemical weathering can reflect the source, weathering rate and impact on climate change [36,37]. The evolution of water chemistry is closely related to the degree of human activity. The transport of waste water, waste and waste gas will bring in more $NO_3{}^{-}$, Cl^{-} and $SO_4{}^{2-}$ plasma and will change the content and concentration of water chemical components [38]. TDS represents the comprehensive characteristics of solute quality in water, with a certain representative value. According to our study, the content of $SO_4{}^{2-}$ decreased in autumn. Bosten Lake is a tourist attraction and if strongly affected by human activities, and there are surrounding salt fields as well as a large number of farmlands. The lake is also subject to industrial wastewater and agricultural backwater. Therefore, this activity plays a role in the ion composition of the lake water, which is one of the main reasons for the rise in the pH value and TDS.

5. Conclusions

The research object of this paper was Bosten Lake. The following conclusions were obtained by using the hydrochemical method. The ionic concentration order of the two seasons was $SO_4{}^{2-} > Cl^{-} > HCO_3{}^{-} > Mg^{2+} > Ca^{2+} > K^{+}$, and the lake water was weakly alkaline. Wei Xing et al. [39], using the Kashi Delta of Xinjiang as their research object, concluded that the highest anion content was $SO_4{}^{2-}$ and the highest cation content was Na^{+}. Tian Yuan et al. [40] used the natural water of Tibet as the research object and concluded that the content of $SO_4{}^{2-}$ was the highest when anions gradually change to $SO_4{}^{2-}$, and the content of Na^{+} was the highest when cations gradually change to Na+, which is consistent with our conclusions. Zeng Xiaoxian et al. [41] concluded that the spatial difference of ions was large by studying the Kashgar River basin in Xinjiang. The concentrations of TDS, Ca^{2+}, Na^{+}, Mg^{2+}, Cl^{-} and $HCO_3{}^{-}$ in Bosten Lake increased significantly in autumn, while the concentrations of K^{+} and $SO_4{}^{2-}$ decreased, thus achieving a similar conclusion to that of Zeng Xiaoxian et al., Luan Fengjiao et al., Shen Beibei et al. and Zhang Jingtao et al. who studied the water chemistry of the surface water or groundwater of rivers and lakes in arid and semi-arid areas by Piper three plot and Gibbs plot, and they concluded that the water chemistry type was SO_4, and the water body was affected by evaporating crystallization and rock weathering [42–44]. In our research, the hydrochemical type (SO_4·Cl-Na·Mg) was the same throughout the lake and in both seasons. In summer, the Great and Little lakes were mainly characterized by evaporation and crystallization, with some rock weathering, and in autumn, evaporation crystallization was dominant in the Great lake, whereas rock weathering is dominant in the Little lake, which is consistent with

their conclusions. Yang Jingyan et al. [45], taking the surface water of the Ilykesh River Basin in Xinjiang as the research object; Zhang Jie et al. [31], using the surface water of Xinjiang Erqiang watershed; and Mengqi [46], analyzing the groundwater of Shiyang River, concluded that cation substitution and the dissolution of carbonate and silicate were the main processes in their study areas. In summer, ions mainly originated from the dissolution of gypsum, salt rock, calcite, dolomite and aragonite, and the excess in Ca^{2+} and $SO_4{}^{2-}$ had other sources. In autumn, ions originated from the dissolution of gypsum, salt rock, calcite and dolomite, and the excess in Ca^{2+} had other sources; cationic alternating adsorption occurs in summer, which is in agreement with previous research.

Author Contributions: X.W. designed the study, conducted the study, analyzed the data and wrote the paper. D.A. played a guiding role and supervised the writing of the paper. S.T. contributed and guided the TDS mapping. All authors have read and agreed to the published version of the manuscript.

Funding: This project was funded by the National Natural Science Foundation Program (41661007, 41261003) and Sci-Tech Innovation and Base Construction Project of Xinjiang, China (NO:2020D04039).

Institutional Review Board Statement: Not applicable.

Informed Consent Statement: Not applicable.

Data Availability Statement: The data presented in this study are available in the article.

Acknowledgments: We thank the five anonymous reviewers for their constructive comments and suggestions that have helped to improve the original manuscript. Thanks are also due to the editorial staff.

Conflicts of Interest: The authors declare no conflict of interest.

References

1. Li, R.; Zhang, F.; Gao, Y. Surface hydrochemistry characteristics and controlling factors in the Ebinur Lake region during dry and wet seasons. *J. Glaciol. Geocryol.* **2016**, *38*, 1394–1403. [CrossRef]
2. Asare-Donkor, N.K.; Ofosu, J.O.; Adimado, A.A. Hydrochemical characteristics of surface water and ecological risk assessment of sediments from settlements within the Birim River basin in Ghana. *Environ. Syst. Res.* **2018**, *7*, 9. [CrossRef]
3. Pu, T. Hydrological Processes Study in a Typical Temperate Glacial Basin Based on Hydrogeochemistry and Isotopes. Ph.D. Thesis, Lanzhou University, Lanzhou, China, 2013.
4. Tang, X.W.; Wu, J.K. Major ion chemistry of surface water in the Xilin River Basin and the possible controls. *Environ. Sci.* **2014**, *35*, 131–142. [CrossRef]
5. Xie, G.J.; Zhang, J.P.; Tang, X.M.; Cai, Y.; Gao, G. Water quality in Bosten Lake (2010–2011) and its evolution trend in recent 50 years. *J. Lake Sci.* **2011**, *23*, 837–846.
6. Zhang, M.; Dilinuer, A.J. Evaluation of ecosystem service value of constructed wetland on the west bank of the Bosten Lake. *Trans. Oceanol. Limnol.* **2021**, *43*, 169–174. [CrossRef]
7. Peng, J.B.; Huang, Y.; Liu, T.; Zhang, Y.; Cheng, Y.; Jiang, L.X. Ecological water requirement of Bosten Lake wetland based on ecosystem service value. *Chin. J. Hydroecol.* **2020**, *41*, 21–30. [CrossRef]
8. Peng, Y.F.; Li, Z.Q.; Yao, X.J.; Mou, J.X.; Han, W.X.; Wang, P.P. Analysis of Bosten Lake area change and its influencing factors based on multi-source remote sensing data and GEE platform. *J. Geo-Inform. Sci.* **2021**, *23*, 1131–1153. [CrossRef]
9. Yang, X. *Assessment of Water Production and Water Quality Purification Services in Arid Areas of Northwest China under the Background of Climate and Land Use Change*; East China Normal University: Shanghai, China, 2020.
10. Nueraminaimu, A. Study on Hydrogen-Oxygen Isotopes and Water Chemistry Characteristics in Bosten Lake Basin. Master's Thesis, Xinjiang University, Ürümqi, China, 2006.
11. Kou, Y.C. Analysis on Water Chemical Characteristics and Influencing Factors of Jinghe River. Master's Thesis, Northwest A & F University, Xianyang, China, 2018.
12. Prasanna, M.V.; Chidambaram, S.; Gireesh, T.V.; Jabir Ali, T.V. A study on hydrochemical characteristics of surface and sub-surface water in and around Perumal Lake, Cuddalore district, Tamil Nadu, South India. *Environ. Earth Sci.* **2011**, *63*, 31–47. [CrossRef]
13. Mandal, A.; Haiduk, A. Hydrochemical characteristics of groundwater in the Kingston Basin, Kingston, Jamaica. *Environ. Earth Sci.* **2011**, *63*, 415–424. [CrossRef]
14. Zhang, J.X.; Zhu, B.Q. Characteristics and influencing factors of hydrochemical composition in northern Xinjiang. *Geogr. Res.* **2022**, *41*, 1437–1458. [CrossRef]

15. Wu, D.D.; Yao, Z.; Jia, F.C.; Wei, X.F.; Sun, H.Y.; Xie, N. Analysis on hydrochemical characteristics and genesis of groundwater in Hami Basin, Xinjiang. *J. Arid Land Resour. Environ.* **2020**, *34*, 133–141. [CrossRef]
16. Dong, X.; Wu, C.Q. Theoretical model, system and method of urban competitiveness evaluation: A literature review. *J. Hubei Univ. Econ.* **2017**, *15*, 66–72. [CrossRef]
17. Kresl, P.K. *The Determinants of Urban Competitiveness: Asurvey, North American Cities and the Global Economy*; Sage Publications: Thousand Oaks, CA, USA, 1995.
18. Zhang, C.; Li, D.; Zhang, J.; Wei, X.M. Evaluation and evolution of urban competitiveness in Northwest China based on principal component analysis. *J. Arid Land Resour. Environ.* **2015**, *29*, 8–13. [CrossRef]
19. Liu, P.; Song, J. Application of city competitiveness evaluation in new urbanization of Beijing-Tianjin-Hebei. *J. Hebei Univ. Econ. Bus.* **2019**, *40*, 65–72. [CrossRef]
20. Zhang, J.X. Study on Competitiveness Evaluation of National Central Cities in Central and Western China. Master's Thesis, Zhengzhou University, Zhengzhou, China, 2019.
21. Dang, Y.P. Research on Comprehensive Evaluation of Urban Competitiveness in Beijing-Tianjin-Hebei. Ph.D. Thesis, Hebei University, Baoding, China, 2019.
22. Gong, X.Y.; Weng, B.S.; Yan, D.H.; Yang, Y.H.; Yan, D.M.; Niu, Y.Z.; Wang, H. Potential recharge sources and origin of solutes in groundwater in the central Qinghai–Tibet Plateau using hydrochemistry and isotopic data. *J. Hydrol. Reg. Stud.* **2022**, *40*, 101001. [CrossRef]
23. Lu, Y. *Application of Multivariate Statistical Method in the Study of Groundwater Hydrochemical Distribution in Zhangye Basin*; Hebei University of Geosciences: Shijiazhuang, China, 2016.
24. Wang, Y. *Land Use Change and Economic Center of Gravity Migration in Bosten Lake Basin*; Xinjiang University: Ürümqi, China, 2015.
25. Mechti, T.A.; Hamidi, I.; Zuppi, Y.M.; Li, J.T. Effects of land use change on ecological service value in Yanqi Basin. *Res. Soil Water Conserv.* **2012**, *19*, 137–141.
26. Ayisulitan, M. *Land Use/Cover Change and Its Driving Factors in Bosten Lake Basin*; Xinjiang Normal University: Urumqi, China, 2014.
27. Wang, L. *Analysis of Runoff Sequence of Main Inflow Rivers in Bosten Lake Basin*; Sichuan Normal University: Chengdu, China, 2008.
28. Ge, Y.; Liu, L.; Gao, Z. Characteristics and geological significance of rare earth elements of Upper Permian in Zhina area. *Shanxi Cok. Coal Sci. Technol.* **2011**, *35*, 16–21.
29. Shen, Y.F.; Ma, H.Y.; Yang, Y.D.; Cao, Y. Evolution characteristics and genesis of shallow fluorine-bearing groundwater in Wuqing Sag. *Geophys. Geochem. Explor.* **2021**, *45*, 528–535. [CrossRef]
30. Sun, H.; Mao, Q.; Wei, X.; Zhang, H.; Xi, Y. Hydrogeochemical characteristics and formation evolutionary mechanism of the groundwater system in the Hami basin. *Geol. China* **2018**, *45*, 1128–1141. [CrossRef]
31. Zhang, J.; Zhou, J.L.; Zeng, Y.Y.; Tu, Z.; Ji, Y.Y.; Sun, Y.; Lei, M. Hydrochemical characteristic and their controlling factors in the Yarkant river basin of Xinjiang. *Environ. Sci.* **2021**, *42*, 1706–1713. [CrossRef]
32. Wu, C.J.; Li, N.; Wang, Y.T.; Ma, Q.M. Application of spatial interpolation method to seawater eutrophication evaluation in Jinzhou Bay. *J. Water Resour. Water Eng.* **2012**, *23*, 116–119.
33. Yang, K.D.; Xie, H.X.; Sui, B. Research on spatial interpolation of rainfall based on GIS: A case study of Hunan Province. *Res. Soil Water Conserv.* **2020**, *27*, 134–138. [CrossRef]
34. Gu, X.M. *Geochemical Characteristics and Genetic Evolution Mechanism of the Alshanquan Group*; China University of Geosciences: Beijing, China, 2018.
35. Hu, C.C. *Research on Distribution Characteristics of Karst Water and Water Chemical Composition in Gugui Mining Area, Huainan*; Anhui University of Science and Technology: Huainan, China, 2018.
36. Gibbs, R.J. Water chemistry of the Amazon River. *Geochim. Cosmochim. Acta* **1972**, *36*, 1061–1066. [CrossRef]
37. Le, J.X.; Wang, D.C. Hydrochemistry of rivers in China. *Acta Geog. Sin.* **1963**, *3*, 3–15. [CrossRef]
38. Zhang, T.; Wang, M.G.; Zhang, Z.Y.; Liu, T.; He, J. But lake basin surface water chemical characteristics and control factors. *J. Environ. Sci.* **2020**, *9*, 4003–4010. [CrossRef]
39. Wei, X.; Zhou, J.L.; Nai, W.H.; Zeng, Y.Y.; Fan, W.; Li, B. Hydrochemical characteristics and evolution of groundwater in the Kashgar Delta Area in Xinjiang. *J. Environ. Sci.* **2019**, *40*, 4042–4051. [CrossRef]
40. Yuan, T.; Qun, Y.; Li, L.K.; Shuang, W.J.; Zhou, Z.X.; Xiang, N.R.; Lei, T.X. Hydrochemical properties and elemental characteristics of natural water in Tibet. *Acta Geogr. Sin.* **2014**, *69*, 969–982. [CrossRef]
41. Zeng, X.X.; Zeng, Y.Y.; Zhou, J.L.; Lu, H. Hydrochemical characteristics and Origin analysis of high sulfate groundwater in Kashgar River Basin, Xinjiang. *Resour. Environ. Arid Areas* **2022**, *4*, 128–135. [CrossRef]
42. Luan, F.J.; Zhou, J.L.; Jia, R.L.; Lu, C.X.; Bai, M.; Liang, H.T. Hydrochemical characteristics and origin of groundwater in Balikun-Yiwu Basin, Xinjiang. *Environ. Chem.* **2017**, *36*, 380–389. [CrossRef]
43. Shen, B.B.; Wu, J.L.; Jili, A.F.; Saparov, A.S.; Isanova, G. The balkhash lake basin water chemical and isotopic space distribution and environmental characteristics. *J. Environ. Sci.* **2020**, *9*, 173–182. [CrossRef]
44. Zhang, J.T.; Shi, Z.M.; Wang, G.C.; Jiang, J.; Yang, B.C. Qaidam basin, the water chemical characteristics and evolution law of groundwater in big had. *Geol. Front* **2021**, *28*, 194–205. [CrossRef]

45. Yang, J.Y.; Yang, Y.H.; Cheng, H.Y.; Cheng, F.X.; Kang, Z.K.; Ping, W.L. Hydrochemical characteristics and possible controls of the surface water in Kashi River Basin, Ili, Xinjiang. *Environ. Chem.* **2021**, *40*, 3815–3827. [CrossRef]
46. Meng, Q. In the middle and lower reaches of shiyang river basin, shallow groundwater hydrochemical characteristics and its formation. *J. Arid Zone Resour. Environ.* **2021**, *35*, 80–87. [CrossRef]